

Galactic Dynamics & Star Clusters

An Overview Lecture for MSc and PhD Students

Matías Blaña

Universidad de La Serena, Chile

November 21, 2025

Introduction

What is Galactic Dynamics?

Galactic dynamics studies the **structure and evolution** of self-gravitating systems, from star clusters to galaxies and dark matter halos.

- ▶ **Gravitational** interactions of many particles ($N \gg 1$).
- ▶ Collisionless vs collisional fluids.
- ▶ Orbits, potentials, instabilities, relaxation, secular evolution.
- ▶ Connection to astrometric, spectroscopic, and photometric observations.

Key questions:

- ▶ How are stars, gas, and dark matter distributed in 3D?
- ▶ What determines their motions (orbits)?
- ▶ How do systems respond to perturbations?
- ▶ What physics governs their long-term evolution?

Why Study Gravitational Dynamics?

Gravity dominates the structural evolution of nearly all astronomical systems:

- ▶ Galaxy formation and substructure.
- ▶ Disk stability: Jeans instability, Toomre Q .
- ▶ 3D orbital families in complex potentials.
- ▶ Secular dynamics and angular-momentum transfer.
- ▶ Gravitational collapse, mergers, stripping, heating.

Direct applications:

- ▶ Dynamical models → mass distribution (baryons + DM).
- ▶ Interpretation of stellar and gas kinematics.
- ▶ Evolution and dissolution of stellar clusters.
- ▶ Reconstruction of orbital histories.
- ▶ Determination of forces, potentials, and gravitational fields.

Introduction

Dynamics across inter-connected scales



Figure: Systems with 10+ orders of magnitude difference in mass and size.

Star Clusters vs Galaxies: Two Regimes

Galaxies: collisionless dynamics

- ▶ $N \sim 10^9 - 10^{12}$ particles.
- ▶ $t_{\text{relax}} \gg t_{\text{Hubble}}$.
- ▶ CBE and smooth potentials dominate.

Stellar clusters: collisional dynamics

- ▶ $N \sim 10^4 - 10^6$.
- ▶ $t_{\text{relax}} \sim 0.01 - 10$ Gyr.
- ▶ Evolution driven by scattering, evaporation, mass segregation.

Both systems share:

- ▶ Self-gravity and gravitational instabilities,
- ▶ Structure and anisotropies,
- ▶ Energy loss and secular evolution.

From Individual Orbits to Collective Physics

Galactic dynamics bridges two scales:

1. Statistical physics of the ensemble

- ▶ Distribution function $f(\mathbf{x}, \mathbf{v})$.
- ▶ Collisionless Boltzmann equation.
- ▶ Moment equations: Jeans equations.
- ▶ Collective instabilities (Jeans, Toomre, bars).

2. Individual orbits

- ▶ Integration of equations of motion.
- ▶ Orbital invariants, frequencies.
- ▶ Resonances.

The bridge between both: the **gravitational potential**.

How We Infer a Galaxy's Gravitational Potential

Central goal: recover $\Phi(x)$ and the underlying mass distribution.

- ▶ **Kinematics:** rotation curves, velocity dispersion.
- ▶ **Photometry:** light profiles → stellar mass distribution.
- ▶ **Gas:** cold tracers (CO, HI), ionized gas.
- ▶ **Cluster and satellite dynamics:** DM halos.
- ▶ **Actions and DFs:** detailed dynamical modeling.

Tools:

- ▶ Jeans equations.
- ▶ N-body simulations, orbit-based methods (Schwarzschild, Made-to-Measure).
- ▶ Analytical models (Plummer, Hernquist, MN, NFW).

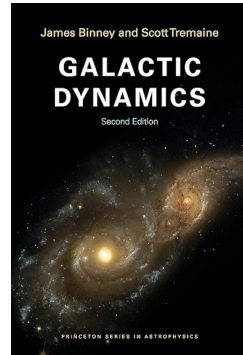
Literature

Books

- ▶ Galactic Dynamics, Binney & Tremaine
2008

Useful web pages:

- ▶ Homepage: van den Bosch
<https://campuspress.yale.edu/vdbosch/teaching/>
- ▶ Homepage: J.Bovy
<https://galaxiesbook.org/>



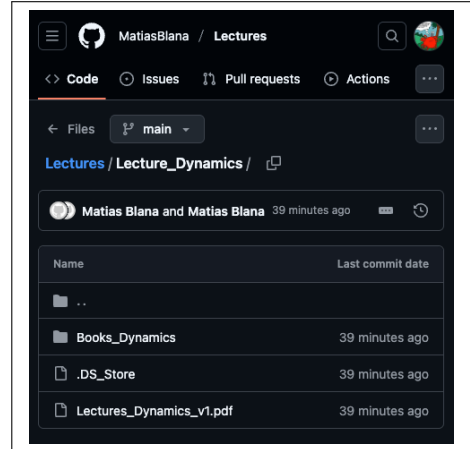
Lecture Material

Repository:

- ▶ Slides in PDF
- ▶ Scripts (Python)

Available in GitHub:

https://github.com/MatiasBlana/Lectures/tree/main/Lecture_Dynamics



Newtonian Gravity and Motion



Reputed descendants of Newton's apple tree at
Trinity College, Cambridge (Wiki)

Newton's Law: Pairwise Force

The Universal Law of gravity describes the forces between two objects, which depend on the **gravitational rest masses** m_1 and m_2 , the distance between them r , and the gravitational constant G :

$$F = G \frac{m_1 m_2}{r^2} \quad (1)$$

Where the gravitational constant is:

$$G = 6.67430 \times 10^{-11} \text{ m}^3 \text{ kg}^{-1} \text{ s}^{-2} \quad (\text{in SI}) \quad (2)$$

$$G = 4.302 \times 10^{-6} \text{ kpc M}_\odot^{-1} (\text{km/s})^2 \quad (\text{useful for galaxies}) \quad (3)$$

$$G = 4\pi^2 \text{ AU}^3 \text{ M}_\odot^{-1} \text{ yr}^{-2} = 39.4784176 \text{ AU}^3 \text{ M}_\odot^{-1} \text{ yr}^{-2} \quad (\text{useful for stars and proto disks}) \quad (4)$$

Vector form (force on m_1 due to m_2):

$$\mathbf{F}_{12} = -G \frac{m_1 m_2}{r^2} \hat{\mathbf{r}}_{12} \quad (5)$$

and force on m_2 due to m_1):

$$\mathbf{F}_{21} = -G \frac{m_1 m_2}{r^2} \hat{\mathbf{r}}_{21} \quad (6)$$

Where we know from Newton's third law:

$$\mathbf{F}_{12} = -\mathbf{F}_{21} \quad (7)$$

Gravitational acceleration field

Similarly, the gravitational (acceleration) field vector form (on m_1 due to m_2):

$$\mathbf{g}_2 = -G \frac{m_2}{r^2} \hat{\mathbf{r}}_{12} \quad (8)$$

and on m_2 due to m_1):

$$\mathbf{g}_1 = -G \frac{m_1}{r^2} \hat{\mathbf{r}}_{21} \quad (9)$$

Where we know from Newton's third law:

$$m_1 \mathbf{g}_2 = -m_2 \mathbf{g}_1 \quad (10)$$

Acceleration, Momentum, Forces

Momentum:

$$\mathbf{p} = m\mathbf{v} \quad (11)$$

Newton's Second Law:

$$\frac{d\mathbf{p}}{dt} = m\mathbf{a} = \mathbf{F} \quad (12)$$

Constant mass:

$$\mathbf{a} = \frac{1}{m} \mathbf{F} \quad (13)$$

Gravity:

$$\mathbf{F}_g = -m_g \mathbf{g} \quad (14)$$

If $m = m_g$ (Equivalence Principle):

$$\mathbf{a} = -\mathbf{g} \quad (15)$$

Lorentz Force (EM):

$$\mathbf{F}_{\text{Lorentz}} = q(\mathbf{E} + \mathbf{v} \times \mathbf{B}) \quad (16)$$

$$\mathbf{a}_{\text{Lorentz}} = \frac{q}{m} (\mathbf{E} + \mathbf{v} \times \mathbf{B}) \quad (17)$$

Ram Pressure:

$$\mathbf{F}_{\text{RP}} = -A \rho_{\text{env}} v^2 \hat{\mathbf{v}} \quad (18)$$

$$\mathbf{a}_{\text{RP}} = \frac{-1}{m} A \rho_{\text{env}} v^2 \hat{\mathbf{v}} \quad (19)$$

Dynamical Friction:

$$\mathbf{a}_{\text{Dyn}} \propto -m \rho_{\text{env}} v^{-2} \hat{\mathbf{v}} \quad (20)$$

Potential Definition and Superposition

Define the gravitational potential per unit mass Φ by

$$\mathbf{g} = -\nabla\Phi \quad (21)$$

Continuous source $\rho(\mathbf{r}')$:

$$\Phi(\mathbf{r}) = -G \int \frac{\rho(\mathbf{r}')}{|\mathbf{r} - \mathbf{r}'|} d^3 r' \quad (22)$$

Point mass M at the origin:

$$\Phi(r) = -\frac{GM}{r} \quad (23)$$

From Field to Poisson's Equation

Start from (21) and take divergence:

$$\nabla \cdot \mathbf{g} = \nabla \cdot (-\nabla \Phi) = -\nabla^2 \Phi \quad (24)$$

Gauss's law for gravity (Newtonian) gives

$$\nabla \cdot \mathbf{g} = -4\pi G \rho \quad (25)$$

Equating (24) and (25) we get Poisson's equation:

$$\nabla^2 \Phi = 4\pi G \rho \quad (26)$$

We also have that the sum of densities is the linear sum of their potentials:

$$\sum_i \nabla^2 \Phi_i = \Phi_{\text{tot}} = \sum_i \rho_i = \rho_{\text{tot}} \quad (27)$$

In vacuum ($\rho = 0$) we get Laplace's equation:

$$\nabla^2 \Phi = 0 \quad (28)$$

Spherical Symmetry: Integrating Poisson

Spherical symmetry $\Rightarrow \Phi = \Phi(r)$:

$$\frac{1}{r^2} \frac{d}{dr} \left(r^2 \frac{d\Phi}{dr} \right) = 4\pi G \rho(r) \quad (29)$$

Integrate once from 0 to r :

$$r^2 \frac{d\Phi}{dr} = G \left[4\pi \int_0^r \rho(r') r'^2 dr' \right] \equiv GM(r) \quad (30)$$

Hence

$$\frac{d\Phi}{dr} = \frac{GM(r)}{r^2}, \quad M(r) = 4\pi \int_0^r \rho(r') r'^2 dr' \quad (31)$$

Solving Poisson's Equation: Overview

We seek the potential generated by a mass density:

$$\nabla^2 \Phi(\mathbf{x}) = 4\pi G \rho(\mathbf{x}) \quad (32)$$

Analytic solutions only exist for simple symmetries:

- ▶ Spherical systems
- ▶ Razor-thin axisymmetric disks
- ▶ Known analytic models (Plummer, Hernquist, MN, NFW)

General galaxies \Rightarrow numerical solvers.

Boundary conditions matter:

- ▶ **Periodic** (cosmological simulations, FFT-based PM codes)
- ▶ **Isolated** (galaxies, star clusters)

Different numerical strategies exist for different geometries and resolutions.

FFT-Based Solvers (Particle–Mesh Methods)

FFT solvers exploit the Fourier-space representation:

$$\hat{\Phi}(\mathbf{k}) = -\frac{4\pi G}{k^2} \hat{\rho}(\mathbf{k})$$

Advantages:

- ▶ Fast: $\mathcal{O}(N \log N)$
- ▶ Excellent for large uniform grids
- ▶ Natural in periodic domains (cosmological boxes)

Limitations:

- ▶ Limited to grid resolution (force softened at cell size)

Used in:

- ▶ PM, P3M, TreePM codes (e.g. Gadget, Enzo, RAMSES Hybrid)
- ▶ Cosmological N-body simulations

Relaxation and Multigrid Solvers

Iterative relaxation methods:

- ▶ Jacobi, Gauss–Seidel, SOR (Successive Over-Relaxation)
- ▶ Update solution locally until convergence
- ▶ Robust but slow: $\mathcal{O}(N^{3/2})$

Multigrid (MG):

- ▶ Combines fine and coarse grids for optimal convergence
- ▶ Speed: $\mathcal{O}(N)$ — fastest known PDE solver

Used in:

- ▶ AMR codes: RAMSES, Athena, FLASH
- ▶ High-resolution galaxy simulations

Tree, TreePM and Method Comparison

Tree solvers:

- ▶ Hierarchical domain decomposition
- ▶ Distant masses approximated by multipole expansion
- ▶ Complexity: $\mathcal{O}(N \log N)$

TreePM hybrids:

- ▶ Short-range forces from Tree
- ▶ Long-range forces from FFT (PM)
- ▶ Used in modern large-volume cosmological codes

Recovering the Field from the Potential

$$\mathbf{g}(\mathbf{r}) = -\nabla\Phi(\mathbf{r}) \quad (33)$$

Cartesian components:

$$\mathbf{g} = \left(-\partial_x\Phi, -\partial_y\Phi, -\partial_z\Phi \right) \quad (34)$$

Collision-less Boltzmann Equation (CBE): connecting gravity and movement

Distribution Function and Equations of Motion

One-particle distribution function $f(\mathbf{x}, \mathbf{v}, t)$: number in $d^3x \times d^3v$ is $fd^3x d^3v$.

Equations of motion under $\Phi(\mathbf{x}, t)$:

$$\dot{\mathbf{x}} = \mathbf{v} \quad (35)$$

$$\dot{\mathbf{v}} = \mathbf{a} = -\nabla\Phi(\mathbf{x}, t) \quad (36)$$

Expanding the Lagrangian Derivative

Total (convective) derivative in phase space:

$$\frac{Df}{Dt} = \frac{\partial f}{\partial t} + \dot{\mathbf{x}} \cdot \nabla_{\mathbf{x}} f + \dot{\mathbf{v}} \cdot \nabla_{\mathbf{v}} f \quad (37)$$

Insert (35)–(36):

$$\frac{Df}{Dt} = \frac{\partial f}{\partial t} + \mathbf{v} \cdot \nabla_{\mathbf{x}} f - (\nabla \Phi) \cdot \nabla_{\mathbf{v}} f \quad (38)$$

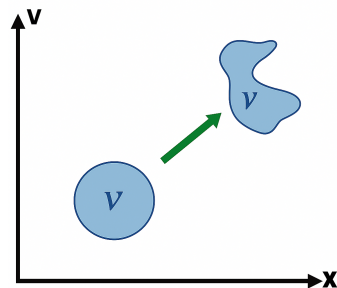
Collisionless Boltzmann Equation (Vlasov)

Liouville's theorem (phase-space incompressibility for Hamiltonian flow):

$$\frac{Df}{Dt} = 0 \iff \frac{\partial f}{\partial t} + \mathbf{v} \cdot \nabla_x f - (\nabla \Phi) \cdot \nabla_v f = 0 \quad (39)$$

This means f is constant along characteristics $(\mathbf{x}(t), \mathbf{v}(t))$.

Note*: collisional systems we have that $\frac{Df}{Dt} = I(t, x, v)$, called the **Fokker–Planck equation**, very hard to solve, but useful for some cases.



CBE: Zeroth Moment (Continuity)

Definitions of Velocity Moments

$$\rho(\mathbf{x}, t) = \int f(\mathbf{x}, \mathbf{v}, t) d^3 v \quad (40)$$

$$\rho u_i = \int v_i f d^3 v \quad (41)$$

$$\rho \langle v_i v_j \rangle = \int v_i v_j f d^3 v \quad (42)$$

Velocity dispersion tensor:

$$\sigma_{ij}^2 \equiv \langle (v_i - u_i)(v_j - u_j) \rangle = \langle v_i v_j \rangle - u_i u_j \quad (43)$$

CBE: Zeroth Moment (Continuity)

Integrate CBE over d^3v

Integrate (39) over velocities and use that $\int \nabla_v \cdot (\dots) d^3v = 0$ if $f \rightarrow 0$ sufficiently fast:

$$\int \frac{\partial f}{\partial t} d^3v + \int v_j \frac{\partial f}{\partial x_j} d^3v = 0 \quad (44)$$

Switch derivatives and integrals:

$$\frac{\partial}{\partial t} \left(\int f d^3v \right) + \frac{\partial}{\partial x_j} \left(\int v_j f d^3v \right) = 0 \quad (45)$$

Hence the continuity equation:

$$\frac{\partial \rho}{\partial t} + \nabla \cdot (\rho \mathbf{u}) = 0 \quad (46)$$

CBE: First Moment (Jeans)

Multiply CBE by v_i and Integrate

Start from (39), multiply by v_i and integrate over d^3v :

$$\frac{\partial}{\partial t} \left(\int v_i f d^3v \right) + \frac{\partial}{\partial x_j} \left(\int v_i v_j f d^3v \right) + \int v_i \left[-\partial_k \Phi \frac{\partial f}{\partial v_k} \right] d^3v = 0 \quad (47)$$

The last term is integrated by parts in v_k :

$$\int v_i (-\partial_k \Phi) \frac{\partial f}{\partial v_k} d^3v = -\partial_k \Phi \int v_i \frac{\partial f}{\partial v_k} d^3v \quad (48)$$

Evaluating the Velocity-Space Surface Term

Use $\int v_i \partial f / \partial v_k d^3 v = [v_i f]_{v_k=-\infty}^{+\infty} - \int \delta_{ik} f d^3 v$. If $v_i f \rightarrow 0$ at $|v_k| \rightarrow \infty$:

$$\int v_i \frac{\partial f}{\partial v_k} d^3 v = - \int \delta_{ik} f d^3 v = -\delta_{ik} \rho \quad (49)$$

Therefore the gravity term in (47) is

$$-\partial_k \Phi (-\delta_{ik} \rho) = +\rho \partial_i \Phi \quad (50)$$

Putting terms together:

$$\frac{\partial(\rho u_i)}{\partial t} + \frac{\partial(\rho \langle v_i v_j \rangle)}{\partial x_j} + \rho \partial_i \Phi = 0 \quad (51)$$

Convective (Jeans) Form and Its Analogy to Euler's Equation

Velocity–moment split:

$$\langle v_i v_j \rangle = u_i u_j + \sigma_{ij}^2 \quad (52)$$

Insert (52) into the first-moment equation (51) and use the continuity equation (46) to obtain:

$$\rho \left(\frac{\partial u_i}{\partial t} + u_j \frac{\partial u_i}{\partial x_j} \right) = - \frac{\partial (\rho \sigma_{ij}^2)}{\partial x_j} - \rho \partial_i \Phi. \quad (53)$$

This is the **Euler-like Jeans momentum equation** for a collisionless stellar fluid, where the tensor $\rho \sigma_{ij}^2$ plays the role of a *pressure/anisotropy stress*.

Comparison with the collisional Euler equation (with gravity):

$$\rho \left(\frac{\partial u_i}{\partial t} + u_j \frac{\partial u_i}{\partial x_j} \right) = - \partial_i P - \rho \partial_i \Phi. \quad (54)$$

Analogy:

$$\boxed{\frac{\partial(\rho \sigma_{ij}^2)}{\partial x_j} \longleftrightarrow \partial_i P}$$

Collisionless systems: anisotropic pressure tensor $\rho \sigma_{ij}^2$ vs. collisional gases: scalar pressure P .

CBE: Second Moment (Dispersion Evolution)

Multiply CBE by $v_i v_j$ and Integrate

Multiply (39) by $v_i v_j$ and integrate:

$$\frac{\partial(\rho \langle v_i v_j \rangle)}{\partial t} + \frac{\partial(\rho \langle v_i v_j v_k \rangle)}{\partial x_k} + \rho (u_i \partial_j \Phi + u_j \partial_i \Phi) = 0 \quad (55)$$

Sketch of gravity term: Integrate by parts twice in v_k , keeping track that $\int v_i v_j \partial f / \partial v_k d^3 v = -\delta_{ik} \int v_j f d^3 v - \delta_{jk} \int v_i f d^3 v$, leading to (55).

Central Moments and the Q_{ijk} Flux

Decompose the third raw moment:

$$\langle v_i v_j v_k \rangle = u_i u_j u_k + u_i \sigma_{jk}^2 + u_j \sigma_{ik}^2 + u_k \sigma_{ij}^2 + Q_{ijk} \quad (56)$$

where the third central moment (heat/dispersion flux) is

$$Q_{ijk} \equiv \langle (v_i - u_i)(v_j - u_j)(v_k - u_k) \rangle \quad (57)$$

Inserting (56) into (55) and using (46), (53) yields:

$$\begin{aligned} & \rho \left(\frac{\partial \sigma_{ij}^2}{\partial t} + u_k \frac{\partial \sigma_{ij}^2}{\partial x_k} + \sigma_{ik}^2 \frac{\partial u_j}{\partial x_k} + \sigma_{jk}^2 \frac{\partial u_i}{\partial x_k} \right) \\ & + \frac{\partial(\rho Q_{ijk})}{\partial x_k} = -\rho(u_i \partial_j \Phi + u_j \partial_i \Phi) + (\text{terms canceled by continuity/Jeans}) \end{aligned} \quad (58)$$

Closure and Physical Meaning

- ▶ The **moment hierarchy** is unclosed: Eq. (58) depends on Q_{ijk} .
- ▶ **Closures** (e.g., $Q_{ijk}=0$, or gradient-diffusion models) are needed for practical modeling.
- ▶ In steady, symmetric systems, many terms simplify, leading to classic Jeans models of galaxies and clusters.

Appendix: Circular Velocity Link (Preview)

Appendix: Circular Velocity Link (Preview)

Centripetal Balance $\Rightarrow v_c - \Phi - M(< r)$

Centripetal acceleration:

$$a_{\text{cent}} = \frac{v_c^2}{r} \quad (59)$$

Gravitational acceleration (spherical):

$$a_r = -\frac{d\Phi}{dr} = -\frac{GM(< r)}{r^2} \quad (60)$$

Circular orbit: set $a_{\text{cent}} = -a_r$:

$$v_c^2(r) = r \frac{d\Phi}{dr} \quad (61)$$

$$v_c^2(r) = \frac{GM(< r)}{r} \quad (62)$$

Summary of Part I

Key Takeaways

- ▶ Newtonian gravity: $\mathbf{a} = -\nabla\Phi$, with $\nabla^2\Phi = 4\pi G\rho$.
- ▶ CBE: $\frac{Df}{Dt} = 0$ encodes phase-space conservation.
- ▶ Moments \Rightarrow continuity (46), Jeans (53), and dispersion evolution (58).
- ▶ The hierarchy requires **closure** (assumptions on higher moments).

Jeans: Spherical Systems

From CBE to Spherical Jeans

Start from the steady, spherical CBE first moment (no $\partial/\partial t$, isotropy not yet assumed). Let $\rho(r)$ be the tracer density, $\overline{v_r^2}(r)$ and $\overline{v_\theta^2}(r) = \overline{v_\phi^2}(r)$ the moments. The radial Jeans equation is

$$\frac{d(\rho \overline{v_r^2})}{dr} + \frac{2\rho}{r} \left(\overline{v_r^2} - \overline{v_\theta^2} \right) = -\rho \frac{d\Phi}{dr}. \quad (63)$$

Define anisotropy

$$\beta(r) \equiv 1 - \frac{\overline{v_\theta^2}}{\overline{v_r^2}}. \quad (64)$$

Divide (63) by ρ to obtain

$$\frac{1}{\rho} \frac{d(\rho \overline{v_r^2})}{dr} + \frac{2\beta \overline{v_r^2}}{r} = - \frac{d\Phi}{dr}. \quad (65)$$

Useful Integral Solution Form

Using (31) ($d\Phi/dr = GM(r)/r^2$) in (65):

$$\frac{d(\rho \bar{v}_r^2)}{dr} + \frac{2\beta \rho \bar{v}_r^2}{r} = -\rho \frac{GM(r)}{r^2}. \quad (66)$$

This linear first-order ODE admits the integrating factor $I(r) = \exp\left(\int \frac{2\beta}{r} dr\right)$, giving

$$\rho \bar{v}_r^2(r) I(r) = \int_r^\infty \rho(s) \frac{GM(s)}{s^2} I(s) ds, \quad \Rightarrow \quad \bar{v}_r^2(r) = \frac{1}{\rho(r)I(r)} \int_r^\infty \rho(s) \frac{GM(s)}{s^2} I(s) ds. \quad (67)$$

For isotropy ($\beta = 0$), $I \equiv 1$.

Isotropic Case and Isothermal Sphere

Isotropy: $\beta = 0 \Rightarrow \overline{v_\theta^2} = \overline{v_r^2}$. Jeans becomes

$$\frac{d(\rho \overline{v_r^2})}{dr} = -\rho \frac{d\Phi}{dr}. \quad (68)$$

Singular isothermal sphere with constant 1D dispersion σ :

$$\rho(r) = \frac{\sigma^2}{2\pi G r^2}, \quad \frac{d\Phi}{dr} = \frac{2\sigma^2}{r}. \quad (69)$$

Then the circular velocity is

$$v_c^2(r) = r \frac{d\Phi}{dr} = 2\sigma^2 = \text{const.} \quad (70)$$

Jeans: Axisymmetric Disks

Jeans in Cylindrical Coordinates (Steady, Axisymmetric)

Assume $\partial/\partial t = 0$ and $\partial/\partial\phi = 0$. The radial and vertical Jeans equations are:

$$\frac{\partial(\rho\bar{v}_R^2)}{\partial R} + \frac{\partial(\rho\bar{v}_R\bar{v}_z)}{\partial z} + \rho \left(\frac{\bar{v}_R^2 - \bar{v}_\phi^2}{R} \right) = -\rho \frac{\partial\Phi}{\partial R}, \quad (71)$$

$$\frac{\partial(\rho\bar{v}_z^2)}{\partial z} + \frac{\partial(\rho\bar{v}_R\bar{v}_z)}{\partial R} + \frac{\rho\bar{v}_R\bar{v}_z}{R} = -\rho \frac{\partial\Phi}{\partial z}. \quad (72)$$

These relate gradients of stress components to the gravitational force.

Thin Isothermal Disk: Vertical Structure (Full Steps)

Assume thin disk near mid-plane with negligible cross term $\overline{v_R v_z} \approx 0$ and $\overline{v_z^2} = \sigma_z^2 = \text{const.}$ From (72):

$$\frac{d(\rho \sigma_z^2)}{dz} = -\rho \frac{d\Phi}{dz}. \quad (73)$$

Combine with Poisson (local sheet):

$$\frac{d^2\Phi}{dz^2} = 4\pi G\rho. \quad (74)$$

Differentiate (73) and use (74):

$$\sigma_z^2 \frac{d^2\rho}{dz^2} = -\rho \frac{d^2\Phi}{dz^2} - \frac{d\rho}{dz} \frac{d\Phi}{dz} = -4\pi G\rho^2 - \frac{d\rho}{dz} \frac{1}{\rho} \frac{d(\rho \sigma_z^2)}{dz}. \quad (75)$$

With $\sigma_z \text{ const}$, an exact solution is the Spitzer sech² profile:

$$\rho(z) = \rho_0 \operatorname{sech}^2\left(\frac{z}{z_0}\right), \quad z_0 = \frac{\sigma_z}{\sqrt{2\pi G\rho_0}}. \quad (76)$$

Radial Force Balance and Asymmetric Drift

From (71) (neglect ∂_z term for an infinitely thin disk in mid-plane):

$$\frac{1}{\rho} \frac{\partial(\rho \bar{v}_R^2)}{\partial R} + \frac{\bar{v}_R^2 - \bar{v}_\phi^2}{R} = - \frac{\partial \Phi}{\partial R}. \quad (77)$$

Define the circular velocity via $v_c^2(R) \equiv R \partial_R \Phi$. Then

$$\bar{v}_\phi^2 = v_c^2 - \bar{v}_R^2 \left[\frac{\partial \ln(\rho \bar{v}_R^2)}{\partial \ln R} + 1 \right]. \quad (78)$$

In terms of \bar{v}_ϕ (assuming small skewness),

$$v_c^2 - \bar{v}_\phi^2 \simeq \bar{v}_R^2 \left[\frac{\partial \ln(\rho \bar{v}_R^2)}{\partial \ln R} + 1 \right]. \quad (79)$$

This lag ($\bar{v}_\phi < v_c$) is the *asymmetric drift* meaning that $\underline{v_c^2 \neq \bar{v}_\phi^2}$.

Exponential Disk: Surface Density and Bessel-Function Formula

Infinitesimally thin exponential disk:

$$\Sigma(R) = \Sigma_0 \exp(-R/R_d). \quad (80)$$

Exact circular velocity (Freeman 1970) with $y = R/(2R_d)$:

$$v_c^2(R) = 4\pi G \Sigma_0 R_d y^2 \left[I_0(y) K_0(y) - I_1(y) K_1(y) \right], \quad (81)$$

where I_n and K_n are modified Bessel functions. The curve rises linearly at small R and peaks near $R \simeq 2.2R_d$.

Including Dispersion: Asymmetric Drift for Disks

If the radial dispersion $\sigma_R(R)$ is non-zero, then $\underline{v_c^2} \neq \underline{v_\phi^2}$ i.e.,

$$v_c^2 - \overline{v_\phi}^2 = \sigma_R^2 \left[\frac{\partial \ln(\Sigma \sigma_R^2)}{\partial \ln R} + 1 \right]. \quad (82)$$

Thus $\overline{v_\phi}$ is lower where σ_R is large and/or declines steeply with R , especially in the inner disk.

Summary of Part II

Key Takeaways

- ▶ Spherical Jeans with anisotropy $\beta(r)$ provides $\overline{v_r^2}(r)$ once $\rho(r)$ and $M(r)$ are given.
- ▶ Axisymmetric Jeans connects stress gradients to $\partial_R\Phi$ and $\partial_z\Phi$; asymmetric drift quantifies $\overline{v_\phi} < v_c$.
- ▶ Exponential disks have closed-form $v_c(R)$ with modified Bessel functions; peak at $\simeq 2.2R_d$.
- ▶ MN disk and NFW halo combine naturally to reproduce flat outer rotation curves.

Common Equilibrium Profiles

Plummer Sphere (Cored)

Density:

$$\rho(r) = \frac{3M}{4\pi a^3} \left(1 + \frac{r^2}{a^2}\right)^{-5/2} \quad (83)$$

Enclosed mass:

$$M(r) = M \frac{r^3}{(r^2 + a^2)^{3/2}} \quad (84)$$

Potential:

$$\Phi(r) = -\frac{GM}{\sqrt{r^2 + a^2}} \quad (85)$$

Circular velocity:

$$v_c^2(r) = \frac{GM r^2}{(r^2 + a^2)^{3/2}} \quad (86)$$

Hernquist (Cuspy)

$$\rho(r) = \frac{M}{2\pi} \frac{a}{r(r+a)^3} \quad (87)$$

$$M(r) = M \frac{r^2}{(r+a)^2} \quad (88)$$

$$\Phi(r) = -\frac{GM}{r+a} \quad (89)$$

$$v_c^2(r) = \frac{GMr}{(r+a)^2} \quad (90)$$

Miyamoto–Nagai Disk (Axisymmetric)

Potential:

$$\Phi(R, z) = -\frac{GM}{\sqrt{R^2 + (a + \sqrt{z^2 + b^2})^2}} \quad (91)$$

Density:

$$\rho(R, z) = \frac{b^2 M}{4\pi} \frac{aR^2 + (a + 3\sqrt{z^2 + b^2})(a + \sqrt{z^2 + b^2})^2}{[R^2 + (a + \sqrt{z^2 + b^2})^2]^{5/2} (z^2 + b^2)^{3/2}} \quad (92)$$

Mid-plane circular velocity:

$$v_c^2(R) = \frac{GMR^2}{[R^2 + (a + b)^2]^{3/2}} \quad (93)$$

NFW Halo (Cosmological)

$$\rho(r) = \frac{\rho_0}{(r/r_s)(1+r/r_s)^2} \quad (94)$$

$$M(r) = 4\pi\rho_0 r_s^3 \left[\ln(1+r/r_s) - \frac{r/r_s}{1+r/r_s} \right] \quad (95)$$

$$\Phi(r) = -4\pi G\rho_0 r_s^3 \frac{\ln(1+r/r_s)}{r} \quad (96)$$

$$v_c^2(r) = \frac{GM(r)}{r} \quad (97)$$

Normalization with concentration $c = r_{200}/r_s$ and ρ_{crit} :

$$\rho_0 = \frac{200}{3} \frac{c^3 \rho_{\text{crit}}}{\ln(1+c) - c/(1+c)}. \quad (98)$$

Common Equilibrium Profiles

Profiles: Summary Table

Model	$\rho(r \rightarrow 0)$	$\rho(r \rightarrow \infty)$	$M(r)$	Notes
Plummer	const. core	r^{-5}	finite $\rightarrow M$	Cored, finite mass
Hernquist	r^{-1}	r^{-4}	finite $\rightarrow M$	Cuspy bulge-like
Miyamoto–Nagai	finite	r^{-3}	—	Flattened disk
NFW	r^{-1}	r^{-3}	log-divergent	Cosmological halo

Composite Rotation Curves (Plummer + MN + NFW)

Composite Rotation Curves (Plummer + MN + NFW)

Total Potential and Circular velocity

Assume total potential as a sum (as we have that $\nabla^2 \sum_i \Phi_i = \Phi_{\text{tot}} = \sum_i \rho_i = \rho_{\text{tot}}$):

$$\Phi_{\text{tot}}(R, z) = \Phi_{\text{Plummer}}(r) + \Phi_{\text{MN}}(R, z) + \Phi_{\text{NFW}}(r), \quad r = \sqrt{R^2 + z^2}. \quad (99)$$

Mid-plane circular velocity adds in quadrature of contributions:

$$v_{c,\text{tot}}^2(R) = v_{c,\text{Plummer}}^2(R) + v_{c,\text{MN}}^2(R) + v_{c,\text{NFW}}^2(R). \quad (100)$$

Where

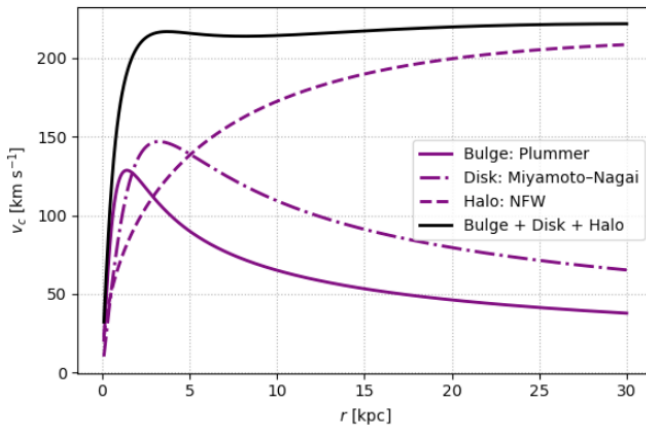
$$v_c^2(R) = \frac{GMR^2}{(R^2 + a^2)^{3/2}}, \quad (101)$$

$$v_{c,\text{MN}}^2(R) = \frac{GM_d R^2}{[R^2 + (a + b)^2]^{3/2}}, \quad (102)$$

$$v_{c,\text{NFW}}^2(R) = \frac{4\pi G\rho_0 r_s^3}{R} \left[\ln(1 + R/r_s) - \frac{R/r_s}{1 + R/r_s} \right]. \quad (103)$$

Composite Rotation Curves (Plummer + MN + NFW)

Figure: Rotation Curves (MN + NFW)



Circular Velocity, Potential Gradient, and Signs

Centripetal Balance and Signs

By definition,

$$a_{\text{cent}} = \frac{v_c^2}{r}, \quad a_r = -\frac{d\Phi}{dr}. \quad (104)$$

Circular orbit requires $a_{\text{cent}} = -a_r$:

$$v_c^2(r) = r \frac{d\Phi}{dr}. \quad (105)$$

For spheres, $d\Phi/dr > 0$ (outward) and force is inward; in ring/disk centers, $d\Phi/dr$ can change sign, implying outward forces near the center.

Where v_c is Meaningful

- ▶ $v_c(r)$ is defined where gravity provides *centripetal* acceleration.
- ▶ In non-spherical potentials (e.g., triaxial halos), closed circular orbits may not exist at all radii; one uses $v_{\text{circ}}(R, 0) = \sqrt{R \partial_R \Phi(R, 0)}$ as a diagnostic.
- ▶ Observed mean rotation $\overline{v_\phi}$ is *not* v_c in general; dispersion reduces $\overline{v_\phi}$ (asymmetric drift).

Virial Ratio and Equilibrium

Virial Theorem

Any gravitational system has a total energy that is the sum of the kinetic and potential energies

$$E = K + U. \quad (106)$$

For a bound isolated system we will have that

$$E = K + U \leq 0. \quad (107)$$

A system is in virial equilibrium if it is in a steady state (or after a long-time average of its moment of inertia $\langle \ddot{I} \rangle = 0$), where its total kinetic and potential energies obey the relation:

$$2K + U = 0. \quad (108)$$

Virial Ratios: Definitions and Meaning

Define

$$\alpha_{\text{vir}} \equiv \frac{2K}{|U|}, \quad Q \equiv \frac{K}{|U|} = \frac{1}{2}\alpha_{\text{vir}}. \quad (109)$$

Virial equilibrium:

$$\alpha_{\text{vir}} = 1 \iff 2K = |U|. \quad (110)$$

Interpretation:

- ▶ $\alpha_{\text{vir}} < 1$: sub-virial \Rightarrow tendency to collapse/contract.
- ▶ $\alpha_{\text{vir}} > 1$: super-virial \Rightarrow tendency to expand/unbind.

Isotropic Systems: Link to Dispersion

For an isotropic system with 1D dispersion σ :

$$K = \frac{3}{2} M \sigma^2. \quad (111)$$

At equilibrium ($2K = -U$):

$$\sigma^2 = \frac{|U|}{3M}. \quad (112)$$

These relations underlie simple dynamical mass estimators.

Examples: Uniform Sphere & Plummer

Uniform-density sphere (M, R):

$$U = -\frac{3}{5} \frac{GM^2}{R}, \quad \sigma^2 = \frac{GM}{5R}. \quad (113)$$

Plummer model (M, a):

$$U = -\frac{3\pi}{32} \frac{GM^2}{a}, \quad \sigma^2 = \frac{\pi}{32} \frac{GM}{a}. \quad (114)$$

The latter is a *global* scaling; local $\sigma(r)$ follows from Jeans.

Observed Virial-Type Estimators

For pressure-supported systems (projected):

$$M \simeq k \frac{R_h \sigma_{\text{los}}^2}{G}, \quad (115)$$

with R_h a characteristic projected radius (often R_e) and k a structure factor ($k \sim 3$ for many spheroids). If ordered rotation contributes, use the second moment

$$\langle v^2 \rangle \rightarrow \langle v_{\text{rot}}^2 + \sigma^2 \rangle. \quad (116)$$

Caveat: k depends on geometry, anisotropy, and light–mass mismatch.

Wolf et al. (2010):

Half-Light Mass

Monthly Notices
of the
ROYAL ASTRONOMICAL SOCIETY

Mon. Not. R. Astron. Soc. **406**, 1220–1237 (2010)



doi:10.1111/j.1365-2966.2010.16753.x

Accurate masses for dispersion-supported galaxies

Joe Wolf,¹★ Gregory D. Martinez,¹ James S. Bullock,¹ Manoj Kaplinghat,¹ Marla Geha,² Ricardo R. Muñoz,² Joshua D. Simon³ and Frank A. Aviles¹

¹*Center for Cosmology, Department of Physics and Astronomy, University of California, Irvine, CA 92697, USA*

²*Astrophysics Department, Yale University, New Haven, CT 06520, USA*

³*Observatories of the Carnegie Institution of Washington, Pasadena, CA 91101, USA*

Accepted 2010 March 27. Received 2010 March 24; in original form 2009 August 22

ABSTRACT

We derive an accurate mass estimator for dispersion-supported stellar systems and demonstrate its validity by analysing resolved line-of-sight velocity data for globular clusters, dwarf galaxies and elliptical galaxies. Specifically, by manipulating the spherical Jeans equation we show that the mass enclosed within the 3D deprojected half-light radius $r_{1/2}$ can be determined with only mild assumptions about the spatial variation of the stellar velocity dispersion anisotropy as long as the projected velocity dispersion profile is fairly flat near the half-light radius, as is typically observed. We find $M_{1/2} = 3G^{-1}\langle n_{\text{gas}}^2 \rangle r_{1/2} \approx 4G^{-1}\langle n_{\text{gas}}^2 \rangle R_e$, where $\langle n_{\text{gas}}^2 \rangle$ is the luminosity-weighted square of the line-of-sight velocity dispersion and R_e is the 2D projected half-light radius. While deceptively familiar in form, this formula is not the virial theorem, which cannot be used to determine accurate masses unless the radial profile of the total mass is known a priori. We utilize this finding to show that all of the Milky Way dwarf spheroidal galaxies (MW dSphs) are consistent with having formed within a halo of a mass of approximately $3 \times 10^7 M_\odot$, assuming a Λ cold dark matter cosmology. The faintest MW dSphs seem to have formed in dark matter haloes that are at least as massive as those of the brightest MW dSphs, despite the almost five orders of magnitude spread in luminosity between them. We expand our analysis to the full range of observed dispersion-supported stellar systems and examine their dynamical I -band mass-to-light ratios $T'_{1/2}$. The $T'_{1/2}$ versus $M_{1/2}$ relation for dispersion-supported galaxies follows a U shape, with a broad minimum near $T'_{1/2} \approx 3$ that spans dwarf elliptical galaxies to normal ellipticals, a steep rise to $T'_{1/2} \approx 3200$ for ultra-faint dSphs and a more shallow rise to $T'_{1/2} \approx 800$ for galaxy cluster spheroids.

<http://dx.doi.org/10.1111/j.1365-2966.2010.16753.x>

Core Result and Why It's Robust

For spherical, dispersion-supported systems with slowly varying $\sigma_{\text{los}}(R)$, **Wolf et al. (2010)** showed the mass at the deprojected half-light radius $r_{1/2}$ is nearly anisotropy-independent:

$$M_{1/2} \equiv M(< r_{1/2}) = \frac{3}{G} \langle \sigma_{\text{los}}^2 \rangle r_{1/2}. \quad (117)$$

Using $r_{1/2} \simeq \frac{4}{3} R_e$ (for typical profiles):

$$M_{1/2} \simeq \frac{4}{G} \langle \sigma_{\text{los}}^2 \rangle R_e. \quad (118)$$

Sketch of the Anisotropy Insensitivity

Spherical Jeans (steady):

$$\frac{d(\nu \bar{v}_r^2)}{dr} + \frac{2\beta \nu \bar{v}_r^2}{r} = -\nu \frac{GM(r)}{r^2}, \quad (119)$$

with tracer density $\nu(r)$ and anisotropy $\beta(r) = 1 - \bar{v}_\theta^2/\bar{v}_r^2$. The *projected* second moment $\langle \sigma_{\text{los}}^2 \rangle$ depends on (ν, β) , but near the radius r_3 where the 3D slope satisfies

$$\left. \frac{d \ln \nu}{d \ln r} \right|_{r=r_3} = -3, \quad (120)$$

the β -dependence cancels to leading order, giving

$$M(r_3) = \frac{3}{G} \langle \sigma_{\text{los}}^2 \rangle r_3. \quad (121)$$

For many light profiles, $r_3 \approx r_{1/2}$, yielding (117).

What Dispersion to Use (Luminosity Weighting)

Define the luminosity-weighted LOS dispersion:

$$\langle \sigma_{\text{los}}^2 \rangle = \frac{\int_0^\infty I(R) \sigma_{\text{los}}^2(R) 2\pi R dR}{\int_0^\infty I(R) 2\pi R dR}, \quad (122)$$

where $I(R)$ is the surface brightness. If $\sigma_{\text{los}}(R)$ is flat near R_e , a single global σ_{los} is a good proxy.

Numerical Forms (Handy Units)

With $G = 4.302 \times 10^{-3}$ pc (km s⁻¹)² M_{\odot}^{-1} :

$$\frac{M_{1/2}}{M_{\odot}} \simeq 930 \left(\frac{\langle \sigma_{\text{los}}^2 \rangle}{(\text{km s}^{-1})^2} \right) \left(\frac{R_e}{\text{pc}} \right), \quad (123)$$

$$\frac{M_{1/2}}{M_{\odot}} \simeq 700 \left(\frac{\langle \sigma_{\text{los}}^2 \rangle}{(\text{km s}^{-1})^2} \right) \left(\frac{r_{1/2}}{\text{pc}} \right). \quad (124)$$

Assumptions and Scope

- ▶ Approximately spherical, dispersion-supported, equilibrium systems.
- ▶ $\sigma_{\text{los}}(R)$ not strongly rising/falling near R_e .
- ▶ Insensitivity to β holds *near* $r_{1/2}$; away from it, anisotropy matters.
- ▶ For rotating systems, include ordered rotation in the second moment if needed:
 $\langle \sigma_{\text{los}}^2 \rangle \rightarrow \langle \sigma_{\text{los}}^2 + v_{\text{rot,los}}^2 \rangle$.

Worked Examples

Worked Examples

Example: Dwarf Galaxy

Given:

$$R_e = 300 \text{ pc}, \quad \langle \sigma_{\text{los}} \rangle = 8 \text{ km s}^{-1}.$$

Using Eq. (123):

$$M_{1/2} \simeq 930 \times (8)^2 \times 300 M_\odot = 1.8 \times 10^7 M_\odot. \quad (125)$$

Mass-to-light inside $r_{1/2}$:

$$\Upsilon_{1/2} \equiv \frac{M_{1/2}}{L_{1/2}} \simeq \frac{2M_{1/2}}{L_{\text{tot}}}. \quad (126)$$

Large $\Upsilon_{1/2}$ indicates dark-matter dominance.

Worked Examples

Example: Ω Centauri (NGC 5139)

Adopt:

$$R_e \simeq 10 \text{ pc}, \quad \langle \sigma_{\text{los}} \rangle \simeq 13 \text{ km s}^{-1}.$$

Projected estimator (Eq. (123)):

$$M_{1/2} \simeq 930 \times 13^2 \times 10 M_\odot \approx 1.57 \times 10^6 M_\odot. \quad (127)$$

Notes:

- ▶ Ω Cen has modest rotation; include v_{rot} if using a second-moment estimator.
- ▶ Uncertainties in R_e and σ_{los} propagate linearly to $M_{1/2}$ in these forms.

When Virial/Wolf Estimators Can Mislead

- ▶ Non-equilibrium (mergers, rapid tides, gas expulsion) $\Rightarrow \langle \ddot{I} \rangle \neq 0$.
- ▶ Strong anisotropy gradients near R_e .
- ▶ Triaxiality or rotation-dominated kinematics without proper second-moment treatment.
- ▶ Mismatch between tracer light and mass distribution (e.g., strong M/L gradients, embedded dark core).

Worked Examples

DRAFT VERSION JANUARY 11, 2022
Typeset using L^AT_EX **twocolumn** style in AASTeX631

nPROFIT: a tool for fitting the surface brightness profiles of star clusters with dynamical models

B. CUEVAS-OTAHOLA,¹ Y. D. MAYYA,¹ I. PUERARI,¹ AND D. ROSA-GONZÁLEZ¹

¹*Instituto Nacional de Astrofísica, Óptica y Electrónica, 72840 Puebla, Mexico*

ACCEPTED AT A^{CEP}

nPROFIT: A TOOL FOR DYNAMICAL MODELS FITTING

15

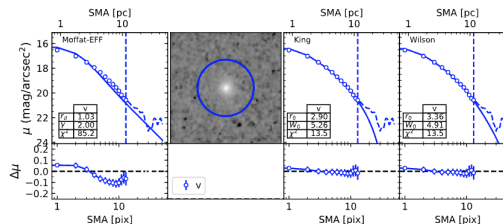


Figure 11. Dynamical models (Moffat-EFF, King and Wilson) fitting performed by nPROFIT to the surface brightness profile of a cluster in the mock sample generated with mksample (top panel). Fitting residuals (bottom panel). The fitting radius is shown with the vertical dashed line, the observed SBP with the empty dots and the fitted models with solid lines.

Figure: Applications of Jeans Equations:

<https://ui.adsabs.harvard.edu/abs/2022arXiv220102881C/abstract>

Dynamical evolution processes in star clusters

Internal Dynamical Processes in Star Clusters

Star clusters evolve through a set of **internal, self-regulated** dynamical mechanisms:

Two-body relaxation

- ▶ Gravitational encounters exchange energy and angular momentum.
- ▶ Pseudo-equilibria: drives an evolution of the initial energy distribution of the system.
- ▶ Sets t_{relax} , t_{evap} , and global evolution.

Scattering and evaporation

- ▶ High-energy encounters eject stars above escape velocity (**gravitational slingshot**).
- ▶ Leads to long-term mass loss ($t_{\text{evap}} \sim 100 t_{\text{relax}}$).

Two-body Scattering, Coulomb Logarithm, and Relaxation time

Context: In a stellar system, stars interact through long-range gravitational forces. Although the mean field dominates the dynamics, **weak, distant encounters** accumulate over time and produce gradual diffusion of energy and angular momentum.

Deflection by a single encounter: For a relative velocity v and impact parameter b , the deflection angle θ is

$$\theta = \frac{2Gm}{bv^2}, \quad (128)$$

valid for small-angle (weak) encounters ($\theta \ll 1$). **(See Binney 2008 for a complete derivation).**

Many-body effect: The cumulative change of velocity from many encounters is obtained by integrating over all possible impact parameters b_{\min} to b_{\max} :

$$\langle(\Delta v)^2\rangle \propto \int_{b_{\min}}^{b_{\max}} \frac{1}{b} db = \ln\left(\frac{b_{\max}}{b_{\min}}\right) \equiv \ln \Lambda. \quad (129)$$

where the **Coulomb logarithm** ($\ln \Lambda$) quantifies the range of impact parameters contributing to cumulative gravitational scattering.

Physical Interpretation of the Coulomb Logarithm

Limits of integration:

- ▶ b_{\min} — the smallest impact parameter, where the deflection becomes large ($\theta \sim 1$):

$$b_{\min} \simeq \frac{Gm}{v^2}. \quad (130)$$

- ▶ b_{\max} — the largest distance over which encounters remain independent, typically of order the system size R or local scale height:

$$b_{\max} \simeq \eta R. \quad (131)$$

Typical value: For star clusters or galaxies, $\ln \Lambda \simeq 10\text{--}20$.

Definition and Physical Meaning of Relaxation Time

The **relaxation time** quantifies how long it takes a stellar system to experience significant energy redistribution due to cumulative weak gravitational encounters. (**See Binney 2008 for a complete derivation**)

Definition:

$$t_{\text{relax}} \simeq \frac{0.1 N}{\ln \Lambda} t_{\text{cross}}, \quad (132)$$

where

- ▶ N is the number of particles (stars),
- ▶ Λ is the **Coulomb parameter**, $\Lambda \simeq b_{\max}/b_{\min} \simeq N$,
- ▶ $t_{\text{cross}} \simeq R/\sigma \simeq R/v_c$ is the dynamical (crossing) time.

Physical meaning:

- ▶ Stars experience many small-angle deflections per crossing.
- ▶ Over $\sim N/(8 \ln \Lambda)$ crossings, their velocity directions change substantially.
- ▶ Relaxation drives the system toward **stationary velocity distribution** (e.g. Maxwellian) and energy equipartition.

Relaxation Times for Different Stellar Systems

Order-of-magnitude examples:

System	N	R [pc]	σ [km/s]	t_{relax} [Gyr]
Open Cluster (e.g. Pleiades)	10^3	3	1	~ 0.1
Globular Cluster (e.g. 47 Tuc)	10^6	10	10	~ 1
Elliptical Galaxy (e.g. M87)	10^{11}	5000	250	$\sim 10^5$
Galaxy Cluster (e.g. Virgo)	10^{13}	10^6	1000	$\sim 10^8$

Scaling behavior:

$$t_{\text{relax}} \propto \frac{N}{\ln N} \frac{R}{\sigma}. \quad (133)$$

Interpretation:

- ▶ Small N and low $\sigma \rightarrow$ short relaxation (collisional regime).
- ▶ Large N and high $\sigma \rightarrow$ long relaxation (collisionless regime).

Collisional vs. Collisionless Regimes

1. **Star clusters (collisional systems):** $t_{\text{relax}} \ll t_{\text{Hubble}}$

- ▶ Two-body encounters drive **core collapse** and **mass segregation**.
- ▶ Energy exchange leads to **evaporation** and tidal loss.

2. **Galaxies (collisionless systems):** $t_{\text{relax}} \gg t_{\text{Hubble}}$

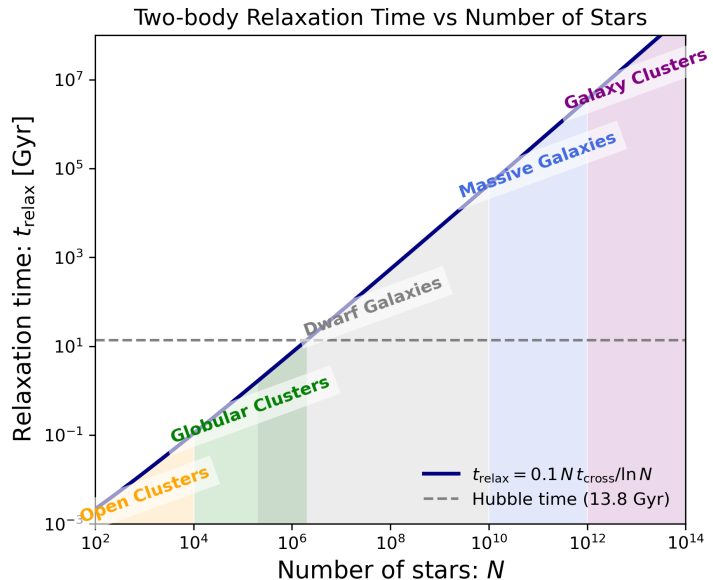
- ▶ Dynamics governed by smooth mean field → **collisionless Boltzmann equation**.
- ▶ Evolution by mergers **violent relaxation**, instabilities, and collective effects (bars, waves).

3. **Galaxy clusters:** $t_{\text{relax}} \gg t_{\text{Hubble}}$

- ▶ Encounters negligible; Relaxation time exceeds age of Universe.
- ▶ But! Relaxation via large-scale **violent relaxation** and **dynamical friction**.

Summary: $t_{\text{relax}}(\text{open cluster}) \ll t_{\text{relax}}(\text{globular}) \ll t_{\text{relax}}(\text{galaxy}) \ll t_{\text{relax}}(\text{cluster})$

Dynamical evolution processes in star clusters



Is Dark Matter Ever Two-body Relaxed?

Setup (Milky Way-like halo):

- ▶ Total dark matter mass $M_{\text{DM}} \simeq 10^{12} M_{\odot}$
- ▶ Crossing time $t_{\text{cross}} \sim \frac{R}{V} \sim 0.2 \text{ Gyr}$ (order-of-magnitude)
- ▶ Two-body relaxation:

$$t_{\text{relax}} \simeq \frac{0.1 N}{\ln N} t_{\text{cross}} \quad (134)$$

Candidate particles and implied N and t_{relax} :

Candidate	Particle mass	Number $N = \frac{M_{\text{DM}}}{m_p}$	t_{relax} [Gyr]
MACHO / PBH	$1 M_{\odot}$	$\sim 10^{12}$	$\sim 7 \times 10^8$
WIMP	$100 \text{ GeV}/c^2$	$\sim 1.1 \times 10^{67}$	$\sim 1 \times 10^{63}$
Axion	$10^{-5} \text{ eV}/c^2$	$\sim 1.1 \times 10^{83}$	$\sim 10^{79}$

Notes: $1 \text{ GeV}/c^2 = 1.7827 \times 10^{-27} \text{ kg}$, $M_{\odot} = 1.9885 \times 10^{30} \text{ kg}$. Numbers use $\ln N$ in Eq. (134) and $t_{\text{cross}} = 0.2 \text{ Gyr}$.

Takeaway: Even in the most “collisional” toy case (all DM as $\sim 1 M_\odot$ black holes), $t_{\text{relax}} \gg$ Hubble time (13.8 Gyr). For particle DM (WIMPs, axions) the implied N makes t_{relax} *astronomically* larger.

Caveats & clarity:

- ▶ Dark matter is (**nearly**) **collisionless** gravitationally: phase-space evolution follows the CBE.
- ▶ Particle *annihilation* (e.g., WIMPs) can produce γ rays, but this is a **particle-physics** process, not two-body *gravitational* relaxation.
- ▶ MACHO/PBH¹-dominated DM is strongly constrained; the table is a **thought experiment**.

¹PBH:primordial black hole

Internal Dynamical Processes in Star Clusters

Mass segregation

- ▶ Energy equipartition causes massive stars/objects to sink to the center.
- ▶ Enhances collisions, binary formation, BH retention.

Core collapse

- ▶ Heat flows outward (gravothermal instability).
- ▶ Core shrinks, density rises; halted by binaries or BH subsystem.

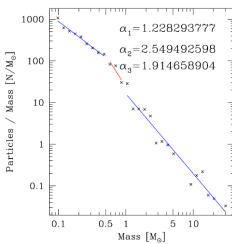
Internal instabilities

- ▶ Radial-orbit instability in anisotropic systems.
- ▶ Collective modes (oscillations, gravothermal breathing).

IMF, Mass Spectrum, and Equipartition

Initial Mass Function (IMF):

- ▶ Clusters are born with a broad mass distribution (Kroupa/Chabrier-like).
- ▶ Typical range: $0.1\text{--}50 M_{\odot}$.
- ▶ Massive stars are rare but dominate energetic encounters.



Energy exchange \Rightarrow equipartition:

$$K_1 = K_2 \quad \Rightarrow \quad \frac{1}{2}m_1v_1^2 = \frac{1}{2}m_2v_2^2$$

Given $m_2 = 4m_1$:

$$v_2 = \frac{v_1}{2}, \quad v \propto m^{-1/2}$$

Consequences:

- ▶ Massive stars lose kinetic energy \Rightarrow sink to center.
- ▶ Low-mass stars gain kinetic energy \Rightarrow move outward.
- ▶ Classical mechanism behind **mass segregation**.

Mass Segregation Simulation

(Download the PDF and open with Adobe Acrobat Reader to play video.)

Mass Segregation Without Equipartition? (Parker et al. 2016)

Classical view:

- ▶ Mass segregation caused by two-body relaxation.
- ▶ Energy equipartition: $mv^2 \approx \text{const.}$
- ▶ Massive stars drift inward as they lose kinetic energy.

Parker et al. (2016):

- ▶ Young clusters can appear mass segregated *before* relaxation can operate.
- ▶ Initial fractal/substructured distributions can collapse and **naturally concentrate massive stars**.
- ▶ Mass segregation may be **primordial**, not equipartition-driven.



Mass segregation in star clusters is not energy equipartition

Richard J. Parker,¹ Simon P. Goodwin,² Nicholas J. Wright,³ Michael R. Meyer⁴ and Sascha P. Quanz⁴

¹Astrophysics Research Institute, Liverpool John Moores University, 146 Brownlow Hill, Liverpool L3 5RF, UK

²Department of Physics and Astronomy, University of Sheffield, Sheffield S3 7RH, UK

³Astrophysics Group, Keele University, Keele, Staffs ST5 5BG, UK

⁴Institute for Astronomy, ETH Zürich, Wolfgang-Pauli-Strasse 27, CH-8093 Zürich, Switzerland

Accepted 2016 March 31. Received 2016 March 31; in original form 2016 March 4

ABSTRACT

Mass segregation in star clusters is often thought to indicate the onset of energy equipartition, where the most massive stars impart kinetic energy to the lower-mass stars and brown dwarfs/free-floating planets. The predicted net result of this is that the centrally concentrated massive stars should have significantly lower velocities than fast-moving low-mass objects on the periphery of the cluster. We search for energy equipartition in initially spatially and kinematically substructured N -body simulations of star clusters with $N = 1500$ stars, evolved for 100 Myr. In clusters that show significant mass segregation we find no differences in the proper motions or radial velocities as a function of mass. The kinetic energies of all stars decrease as the clusters relax, but the kinetic energies of the most massive stars do not decrease faster than those of lower-mass stars. These results suggest that dynamical mass segregation – which is observed in many star clusters – is not a signature of energy equipartition from two-body relaxation.

Key words: methods: numerical – stars: formation – open clusters and associations: general.

Parker et al. 2016, MNRAS 459, L119

<http://arxiv.org/abs/1604.00394>

Cluster Evaporation by Stellar Encounters

Cluster Evaporation through Stellar Scattering

Gravitational encounters between stars lead not only to energy exchange (relaxation) but also to the **escape of stars** from the cluster once their velocities exceed the escape speed.

Mechanism:

- ▶ Two-body gravitational encounters cause small velocity perturbations $\Delta\mathbf{v}$.
- ▶ Over many crossings, these accumulate to a random walk in energy.
- ▶ Stars that gain sufficient kinetic energy ($E > 0$) eventually leave the system.

Escape condition:

$$\frac{1}{2}mv^2 > |E_{\text{bind}}| \Rightarrow v > v_{\text{esc}} = \sqrt{2|\Phi(r)|}. \quad (135)$$

Evaporation timescale: Only a small fraction of stars per relaxation time acquire escape energy. The cluster **evaporation timescale** is empirically

$$t_{\text{evap}} \simeq \zeta t_{\text{relax}}, \quad \zeta \sim 100\text{--}300, \quad (136)$$

where t_{relax} is the two-body relaxation time.

Environmental Dynamical Processes Acting on Clusters

Clusters also evolve due to **external forces** from their host galaxy:

Tidal stripping

- ▶ Stars beyond the tidal radius become unbound.
- ▶ Strong in pericenter passages; produces **tidal tails/streams**.

Tidal heating / compression / shocking

- ▶ Disk crossings, bulge passages, GMC encounters inject energy.
- ▶ Can puff up or compress the cluster depending on geometry.

External tidal fields

- ▶ Shape cluster structure and tidal boundary.
- ▶ Impose non-spherical equipotential surfaces (Roche lobes).

Tidal Stripping and the Jacobi (Hill) Radius

Tidal stripping occurs when a satellite (cluster or dwarf galaxy) orbits inside the potential of a more massive host. Stars beyond a critical radius become unbound due to the host's tidal field.

Jacobi (Hill) radius for a satellite of mass m orbiting a host of mass $M(< R)$:

$$r_J = R \left(\frac{m}{3M(< R)} \right)^{1/3}, \quad (137)$$

derived in the rotating frame by balancing:

$$\text{gravity of satellite} = \text{tidal} + \text{centrifugal forces.}$$

This radius is also called the **tidal radius** or **Hill radius**.

King-model “tidal radius” is different:

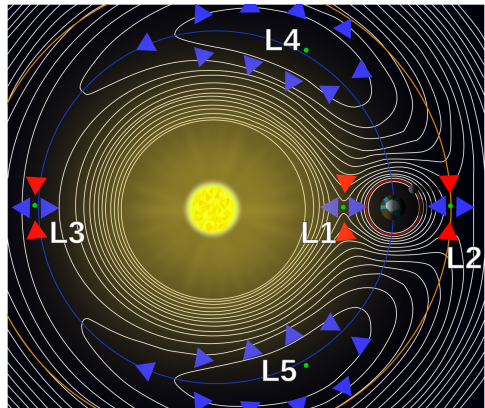
- ▶ The King *tidal radius* (r_t^{King}) is a free parameter from surface-brightness profile fitting.
- ▶ It does *not* necessarily correspond to the dynamical Jacobi radius.
- ▶ r_t^{King} often *overestimates* the true dynamical truncation radius.

Lagrange Points and the Tidal Boundary

In the rotating frame of a satellite orbiting a host galaxy, the effective potential has five equilibrium points, the **Lagrange points**:

- ▶ Inner (L_1) and outer (L_2) saddle points (escape channels). Tidal arms are generated from here, that can be leading (L_1) or trailing (L_2).
- ▶ L_3 : Opposite side of host; minor role.
- ▶ L_4 : Leading triangular point (quasi-stable, Trojans(Greeks)).
- ▶ L_5 : Trailing triangular point (quasi-stable, Trojans).

Key idea: L_1 and L_2 define the **Jacobi radius** and dominate tidal stripping.



Source:Wiki

Modern perspective: Tidal truncation depends on the **full tidal tensor**, orbital phase, mass distribution, and pericentric passages.

Reference: Blaña et al. (2025), *Tidal truncation of satellite galaxies in realistic cluster potentials*.

<https://ui.adsabs.harvard.edu/#abs/2025AA...699A..69B/abstract> We show that the effective tidal radius differs from simple Jacobi estimates and evolves strongly along the orbit.

Tidal Stripping Simulation

(Download the PDF and open with Adobe Acrobat Reader to play video.)

Tidal Shocking of Star Clusters

When a star cluster passes rapidly through a region where the gravitational field changes steeply (e.g., pericentre, disk crossing, bar passage), its stars receive an ****impulsive energy injection**** ("tidal shock").

Energy gain per unit mass in the impulsive approximation (adapted from [Hammer et al. 2024, MNRAS, 527, 2718](#)):

$$\Delta E = \frac{4}{3} \eta \left(\frac{GM_{\text{Host}}(R_{\text{peri}})}{R_{\text{peri}}^2} \right)^2 \left(\frac{r_{\text{rms}}}{V_{\text{peri}}} \right)^2, \quad (138)$$

where: V_{peri} = cluster orbital velocity at pericentre, r_{rms} = 3D rms radius of the stellar system, η accounts for deviations from the ideal impulsive limit.

Physical consequences:

- ▶ Cluster expands after each shock.
- ▶ Repeated shocking accelerates mass loss and can trigger disruption.

Extreme Tidal Shocking (Disruption Limit)

In the most extreme scenario, when the impulsive tidal energy input from the host (Milky Way) equals the binding energy per unit mass of a stellar system ($K/M = \frac{3}{2}\sigma^2$), the tidal shocking reaches the **disruption limit**. Combining equations for ΔE , and $r_{\text{rms}}^2 = 3r_{\text{half,3D}}^2$, and $r_{\text{half,3D}} = 4/3 r_{\text{half}}$ yields the disruption-condition:

$$\frac{\sigma^2}{r_{\text{half}}^2} = \frac{128}{27} \eta \left(\frac{g_{\text{host}}(R_{\text{peri}})}{V_{\text{peri}}} \right)^2, \quad (139)$$

where: σ = one-dimensional velocity dispersion of the satellite (dwarf or star cluster), V_{peri} = orbital velocity at pericentre, the gravitational field $g_{\text{host}}(R_{\text{peri}}) = GM_{\text{host}}(R_{\text{peri}}) R_{\text{peri}}^{-2}$, and η encodes deviations from a pure impulsive shock.

Interpretation: clusters with low σ and large r_{half} are highly vulnerable to tidal disruption during pericentre passages.

Tidal Stripping Simulation: tidal shock

(Download the PDF and open with Adobe Acrobat Reader to play video.)

Environmental Dynamical Processes Acting on Clusters

Dynamical friction

- ▶ Clusters lose orbital energy to the background stellar/DM field.
- ▶ Leads to orbital decay into the galactic center (Bulge NSCs).

Ram pressure (gas-rich environments)

- ▶ Relevant in gas-rich hosts or during early formation.
- ▶ Removes gas; affects embedded cluster survival.

Orbital dynamics

Orbital Dynamics: Overview

Orbital dynamics studies the motion of test particles or stars in a prescribed gravitational potential $\Phi(\mathbf{x})$.

Key ingredients:

- ▶ The potential $\Phi(\mathbf{x}, t)$ (static or rotating).
- ▶ Integration of equations of motion:

$$\dot{\mathbf{x}} = \mathbf{v}, \quad \dot{\mathbf{v}} = -\nabla\Phi.$$

- ▶ Conserved quantities (energy, angular momentum) depending on symmetry.
- ▶ Classification of orbits (tubes, boxes, resonant families).

Applications: galaxy disks, bars, halos, globular clusters, streams, tidal disruption, dark-matter halos.

Analytical Potentials Commonly Used

Plummer Sphere:

$$\Phi(r) = -\frac{GM}{\sqrt{r^2 + a^2}}. \quad (140)$$

Hernquist or NFW Halo:

$$\rho_{\text{NFW}}(r) = \frac{\rho_s}{(r/r_s)(1+r/r_s)^2}. \quad (141)$$

Miyamoto–Nagai Disk:

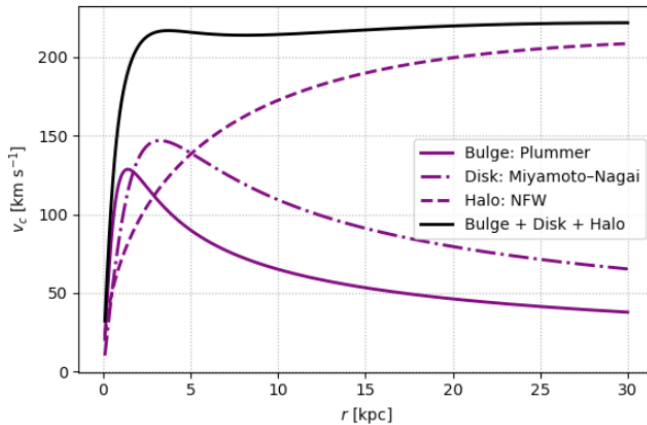
$$\Phi(R, z) = -\frac{GM}{\sqrt{R^2 + \left(a + \sqrt{z^2 + b^2}\right)^2}}. \quad (142)$$

Use cases:

- ▶ Plummer → star clusters, or galaxy bulges
- ▶ MN → thin/thick stellar disks
- ▶ NFW → Λ CDM halos

Orbital dynamics

Figure: Rotation Curves (MN + NFW)



Computing Orbits: Leapfrog and Symplectic Methods

Equations of motion:

$$\dot{\mathbf{x}} = \mathbf{v}, \quad \dot{\mathbf{v}} = -\nabla\Phi.$$

Leapfrog (Kick–Drift–Kick): a symplectic integrator:

$$\mathbf{v}_{n+1/2} = \mathbf{v}_n + \frac{\Delta t}{2} \mathbf{a}(\mathbf{x}_n), \quad (143)$$

$$\mathbf{x}_{n+1} = \mathbf{x}_n + \Delta t \mathbf{v}_{n+1/2}, \quad (144)$$

$$\mathbf{v}_{n+1} = \mathbf{v}_{n+1/2} + \frac{\Delta t}{2} \mathbf{a}(\mathbf{x}_{n+1}). \quad (145)$$

Why leapfrog?

- ▶ Symplectic \rightarrow conserves energy better over long times (Hamiltonian canonical transformation: kinetic and potential operators).
- ▶ Ideal for galaxy and cluster dynamics.

Choosing Δt : at least 1/10 of the crossing/orbital time (depends on velocity and acceleration as well).

Conserved Quantities in Different Potentials

In spherical potentials $\Phi = \Phi(r)$:

- ▶ Energy E conserved.
- ▶ Angular momentum vector \mathbf{L} conserved.
- ▶ Motion confined to a plane.

In axisymmetric potentials $\Phi(R, z)$:

- ▶ Energy E conserved.
- ▶ Only L_z conserved.
- ▶ Tube orbits: short-axis or long-axis tubes.

Orbit Families in Galactic Potentials

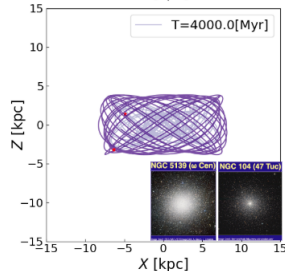
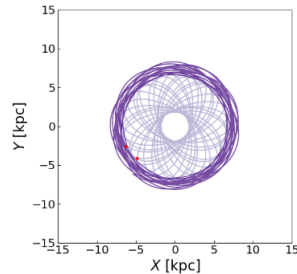
Different potentials support different orbit types:

Spherical Potentials:

- ▶ 1D radial + angular oscillation.
- ▶ Rosette orbits (not closed)
- ▶ Closed orbits only for special potentials (Kepler, Isochrone, Harmonic).

Axisymmetric disk potentials:

- ▶ Tube, and short-axis tubes.



Barred Potentials and Rotating Frames

Galactic bars require a **rotating** non-axisymmetric potential:

$$\Phi(R, \phi, z, t) = \Phi(R, \phi - \Omega_p t, z).$$

Examples of bar potentials:

- ▶ Long & Murali (1992) bar.
- ▶ Dehnen bar potential.
- ▶ **Portail 2017, Sormani et al. (2022)** Milky Way bar (state-of-the-art).

Orbital families in bars:

- ▶ x_1 family (supports the bar).
- ▶ x_2 family (inner perpendicular orbits).
- ▶ Higher-order resonances (Banana, pretzel, etc.) build the box/peanut bulges
- ▶ **Chaotic orbits** appear in triaxial or barred galaxies.

In rotating frames (bars): the **Jacobi energy** E_J is conserved:

$$E_J = E - \Omega_p L_z$$

Codes for Orbit Integration

DELOREAN (Blaña et al. 2020+):

- ▶ Multi-component galaxy potentials.
- ▶ Leapfrog integrator, cosmic expansion motion equations.
- ▶ Python code, parallel orbit sampling, clusters + galaxies.

GALPY (Bovy 2015):

- ▶ Large library of analytic potentials.
- ▶ Orbit integration, actions, distribution functions.
- ▶ Python, widely used.

AGAMA (Vasiliev 2018):

- ▶ Fast action-angle methods.
- ▶ Self-consistent models, Schwarzschild.
- ▶ C++, Python bindings.

Example Orbit Computed with DELOREAN

Model parameters:

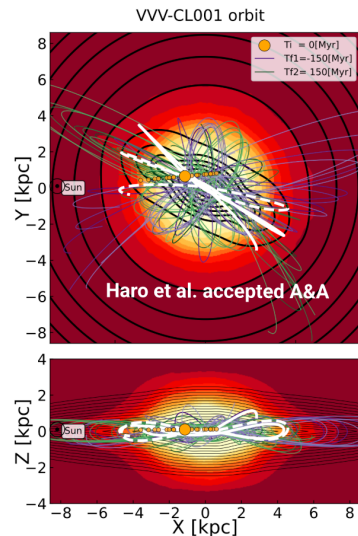
- ▶ Disk: Miyamoto–Nagai (M , a , b).
- ▶ Halo: NFW (ρ_s , r_s).
- ▶ Bulge: Hernquist (M_b , a_b).
- ▶ Pattern speed (bar): Ω_p .

Orbit characteristics:

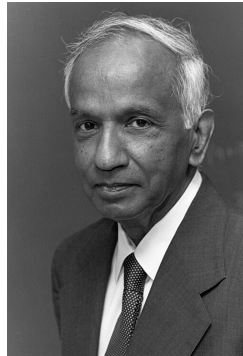
- ▶ Energy $E = \dots$
- ▶ $L_z = \dots$
- ▶ Resonance: x_1 / tube / box.

Reference: Blaña et al. 2020 MNRAS 497,
DELOREAN.

Example of a star cluster orbit integrated in DELOREAN in a
Milky Way potential with a bar, disk, gas, and dark matter halo.



Chandrasekhar's Dynamical Friction



Subrahmanyan Chandrasekhar (Wiki)

Chandrasekhar's Dynamical Friction

Context: A massive object of mass M moves through a sea of lighter background particles of density ρ and isotropic velocity distribution $f(v)$. Gravitational encounters with these particles deflect them and produce a density enhancement (a gravitational wake) behind M , which exerts a drag force opposing its motion.

Physical interpretation:

- ▶ Each encounter transfers a small amount of momentum.
- ▶ The cumulative effect of many weak encounters produces a net deceleration.
- ▶ This process is **collisionless** but arises from long-range gravity.

$$\frac{d\vec{v}_M}{dt} = -4\pi G^2 M \rho \ln \Lambda \frac{\mathbf{v}_M}{v_M^3} \left[\text{erf}(X) - \frac{2X}{\sqrt{\pi}} e^{-X^2} \right] \quad \text{with } X \equiv \frac{v_M}{\sqrt{2}\sigma} \quad (147)$$

Parameters: M — mass of the perturber, ρ — local density of background particles, σ — 1D velocity dispersion of background, $\ln \Lambda$ — Coulomb logarithm, $\Lambda = b_{\max}/b_{\min}$.

Interpretation and Scaling of Dynamical Friction

Key insights:

- ▶ The drag force $\propto M^2$: more massive objects decelerate faster.
- ▶ The term in brackets of Eq. (147) accounts for the fraction of background particles slower than v_M .
- ▶ For $v_M \gg \sigma$: only slow particles contribute \Rightarrow friction $\propto 1/v_M^2$.
- ▶ For $v_M \lesssim \sigma$: nearly all particles contribute \Rightarrow friction saturates.

Energy loss rate:

$$\frac{dE}{dt} = M \mathbf{v}_M \cdot \frac{d\mathbf{v}_M}{dt} \simeq -4\pi G^2 M^2 \rho \ln \Lambda \frac{1}{v_M} \left[\text{erf}(X) - \frac{2X}{\sqrt{\pi}} e^{-X^2} \right] \quad (148)$$

Characteristic decay timescale:

$$t_{\text{df}} \sim \frac{v_M^3}{4\pi G^2 M \rho \ln \Lambda} \quad (149)$$

Interpretation: for a satellite galaxy or massive black hole orbiting in a galactic halo, t_{df} gives

Physical Picture of the Gravitational Wake

The gravitational wake:

- ▶ The moving mass M deflects background particles, leaving an overdensity trailing behind it.
- ▶ The combined gravitational pull of this wake acts as a **drag force**.
- ▶ The direction of the friction is opposite to \vec{v}_M .

Coulomb logarithm:

$$\ln \Lambda = \ln \left(\frac{b_{\max}}{b_{\min}} \right) \quad (150)$$

- ▶ b_{\max} : maximum impact parameter (system scale),
- ▶ b_{\min} : minimum (set by strong deflection limit).

Exercise 1: Proper Motion \rightarrow Tangential Velocity

Consider Omega Centauri with:

$$D_{\Omega\text{Cen}} \simeq 5.2 \text{ kpc}, \quad \mu \simeq 8 \text{ mas/yr.}$$

Tasks:

- (a) Derive the relation between proper motion μ (mas/yr), distance D (kpc), and tangential velocity V_{\tan} (km/s).
- (b) Compute V_{\tan} for:

$$D = 5.2, 52, 520 \text{ kpc}$$

assuming the *same* proper motion $\mu = 8 \text{ mas/yr.}$

Goal: see how the *same* μ corresponds to very different V_{\tan} at different distances.



Omega Centauri (Wiki, ESO)

Exercise 1: Solution and Distance Scaling

The standard conversion is

$$V_{\tan} \text{ [km/s]} = 4.74 \mu \text{ [mas/yr]} D \text{ [kpc]}. \quad (151)$$

For $\mu = 8$ mas/yr:

$$D = 5.2 \text{ kpc} : \qquad V_{\tan} \simeq 4.74 \times 8 \times 5.2 \approx 197 \text{ km/s}, \quad (152)$$

$$D = 52 \text{ kpc} : \qquad V_{\tan} \simeq 10 \times 197 \approx 2000 \text{ km/s}, \quad (153)$$

$$D = 520 \text{ kpc} : \qquad V_{\tan} \simeq 100 \times 197 \approx 2.0 \times 10^4 \text{ km/s}. \quad (154)$$

Key point: a given proper motion corresponds to a tangential velocity that scales linearly with distance.

In practice: use `astropy.coordinates.SkyCoord` to convert between distance, proper motions, and 3D velocities.

Exercise 2: From σ_{los} to Proper-Motion Dispersion

For Omega Centauri, take approximate values:

$$D \simeq 5.2 \text{ kpc}, \quad \sigma_{\text{los}} \simeq 13 \text{ km s}^{-1}.$$

Assume:

- ▶ The velocity distribution is approximately isotropic, so the tangential dispersion is similar:
 $\sigma_t \approx \sigma_{\text{los}}$.
- ▶ You observe a sample of member stars in proper motion.

Tasks:

- (a) Write the relation between σ_t (km/s), D (kpc), and the proper-motion dispersion σ_μ (mas/yr).
- (b) Estimate σ_μ for Omega Centauri.

Exercise 2: Solution (Omega Cen Sample)

Use the same conversion, applied to the *dispersion*:

$$\sigma_\mu \text{ [mas/yr]} = \frac{\sigma_t \text{ [km/s]}}{4.74 D \text{ [kpc]}}, \quad (155)$$

with $\sigma_t \approx \sigma_{\text{los}} = 13 \text{ km/s}$ and $D = 5.2 \text{ kpc}$.

$$\sigma_\mu \approx \frac{13}{4.74 \times 5.2} \approx 0.53 \text{ mas/yr.} \quad (156)$$

Interpretation:

- ▶ The proper motions of member stars should have a spread of $\sim 0.5 \text{ mas/yr}$ due to internal motions.
- ▶ This can be directly compared with Gaia or HST proper-motion uncertainties when modeling the cluster's dynamics.

Again: `astropy.coordinates.SkyCoord` can perform these conversions with full 3D geometry and reference frames.

Exercise 3: Gaia DR3 vs Internal Motions of Omega Cen

From the previous exercise, Omega Centauri has an internal proper-motion dispersion of order:

$$\sigma_{\mu}^{(\text{int})} \sim 0.5 \text{ mas/yr.}$$

Assume that for bright cluster members in Gaia DR3 the typical 1D proper-motion uncertainty is:

$$\sigma_{\mu}^{(\text{Gaia})} \sim 0.05 \text{ mas/yr.}$$

Tasks:

- (a) Compute the signal-to-noise ratio (SNR) for detecting internal motions in *one* star:

$$\text{SNR}_{\star} = \frac{\sigma_{\mu}^{(\text{int})}}{\sigma_{\mu}^{(\text{Gaia})}}.$$

- (b) If you average over N stars, the error on the *mean* motion scales as $\sigma_{\mu}^{(\text{Gaia})}/\sqrt{N}$. For $N = 100$, what is the SNR on the mean?
- (c) Qualitatively: is Gaia DR3 sufficient to resolve the internal kinematics of Omega Cen?

Exercise 3: Solution and Interpretation

(a) Single-star SNR:

$$\text{SNR}_\star = \frac{\sigma_\mu^{(\text{int})}}{\sigma_\mu^{(\text{Gaia})}} \approx \frac{0.5}{0.05} \approx 10.$$

So each bright member has internal motions detected at $\sim 10\sigma$.

(b) SNR of the mean for $N = 100$ stars:

$$\sigma_{\mu, \text{mean}}^{(\text{Gaia})} = \frac{\sigma_\mu^{(\text{Gaia})}}{\sqrt{N}} = \frac{0.05}{\sqrt{100}} = 0.005 \text{ mas/yr},$$

$$\text{SNR}_{\text{mean}} = \frac{\sigma_\mu^{(\text{int})}}{\sigma_{\mu, \text{mean}}^{(\text{Gaia})}} \approx \frac{0.5}{0.005} \approx 100.$$

(c) Interpretation:

- ▶ Gaia DR3 can resolve internal kinematics of Omega Cen with very high significance.
- ▶ Combining many stars allows detailed mapping of velocity-dispersion profiles, rotation, and anisotropy.
- ▶ In practice, one must also account for systematics, crowding, and membership selection.

Summary of Today's Lecture

- ▶ Star clusters evolve under the combined influence of their **internal dynamics** (two-body relaxation, scattering, evaporation, mass segregation, core collapse).
 - ▶ Their evolution is strongly shaped by the **external galactic potential**: disc, bulge, halo, bar, and dark-matter distribution.
 - ▶ We explored **orbital dynamics** of clusters in galaxies: conserved quantities, orbital families, axisymmetric vs. barred potentials, Jacobi energy, tidal shocks, and orbital decay.
 - ▶ The **Jeans equations**, CBE, and Poisson equation provide the theoretical backbone for understanding their kinematics and structural evolution.
 - ▶ Numerical tools (leapfrog integrators, N-body, galpy, AGAMA, Delorean) allow us to model cluster orbits, tidal fields, and long-term survival.

Key Takeaways

- ▶ **Star clusters are dynamical laboratories:** their structure and evolution trace the physics of relaxation, mass segregation, and tidal stripping.
- ▶ A cluster's fate is governed by its **orbit in the host galaxy:** eccentricity, pericenter, inclination, bar resonances, and disc crossings determine the strength of tidal forces.
- ▶ **Galactic tides** sculpt clusters: tidal truncation, shocks, heating, and the formation of streams and extra-tidal stars.
- ▶ Understanding cluster orbits is essential to reconstruct their **formation sites**, migration within the galaxy, and eventual dissolution.
- ▶ With modern surveys (Gaia, HST, JWST, ALMA), we can now combine 6D data, orbits, and dynamical modeling to uncover the **life cycle of star clusters** in the Milky Way and beyond.

Star Clusters = Internal Physics + Galactic Environment

Thank You Very Much!

Galactic Dynamics & Star Clusters

An Overview Lecture for MSc and PhD Students

Matías Blaña

Universidad de La Serena, Chile